2-1-2012

Frequency specific deficits in schizophrenia

Anil Reddy Geeda

Anil Reddy Geeda
Candidate

Electrical and Computer Engineering
Department

This thesis is approved, and it is acceptable in quality and form for publication:

Approved by the Thesis Committee:

Dr. Vince D. Calhoun , Chairperson

Dr. Julia M. Stephen

Dr. Nasir Ghani

FREQUENCY SPECIFIC DEFICITS IN SCHIZOPHRENIA

by

ANIL REDDY GEEDA

BACHELOR OF TECHNOLOGY IN ELECTRONICS
AND
COMMUNICATION ENGINEERING
2009

THESIS

Submitted in Partial Fulfillment of the
Requirements for the Degree of

Master of Science
Computer Engineering

The University of New Mexico
Albuquerque, New Mexico

DECEMBER, 2011

ACKNOWLEDGEMENT

Firstly, I am very much indebted to Dr. Julia M. Stephen and Dr. Vince D. Calhoun for providing me with motivation and encouragement throughout the course of my work. Their breadth of knowledge and enthusiasm has been invaluable. Without their supervision and guidance, I would not be able to complete my thesis.

I would also like to thank Tongsheng Zhang and Brian Coffman for their valuable suggestions and for the many intuitive discussions we had.

I am also thankful to Dr. Nasir Ghani for his encouragement and support.

I am highly indebted to my Father, Ramana Reddy Geeda and my mother, Vanaja Geeda for their affection, motivation and encouragement to pursue a Master’s degree.

FREQUENCY SPECIFIC DEFICITS IN SCHIZOPHRENIA

by

Anil Reddy Geeda

B.TECH., Electronics and Communication Engineering, VIT University, 2009

M.S., Computer Engineering, University of New Mexico 2011

ABSTRACT

Coherence estimation is one of the methods for understanding functional connectivity deficits and frequency specific deficits in schizophrenia. Coherence between different lobes of the brain from task related data at different frequency bands was investigated in patients with Schizophrenia (SP) and Healthy Normal Volunteers (HNV). The task was aimed to study the neural mechanisms underlying auditory and visual integration in patients with schizophrenia relative to healthy controls, which requires intact connectivity between the lobes of the brain in order to recombine the sensory information into a complete percept of the external world. Coherence was calculated from the processed magneto-encephalography (MEG) data for each pair of lobes of left temporal and parietal, left temporal and occipital, right temporal and parietal, right temporal and occipital, parietal and occipital at the frequency bands of delta (0 to 4 Hz), theta (4 -8 Hz), alpha (8-13 Hz), beta (13 -30 Hz) and gamma (30-100 Hz).

Analysis Of Variance (ANOVA) was performed on the coherence data of 30 subjects comprised of 15 patients and 15 controls. There was a significant interaction between

frequency and diagnosis with age. Significant differences were found between patients and controls at the Delta frequency band, which was confirmed with Bonferroni-corrected -t-tests at the delta frequency range in each pair of regions. It was found that patients had higher coherence than controls in the delta frequency band and it was significant across lobes which suggest an abnormal MEG coherence during evoked activity in schizophrenic patients.

TABLE OF CONTENTS

LIST OF FIGURES

LIST OF TABLES

LIST OF ABBREVIATIONS AND ACRONYMS

fMRI	Functional Magnetic Resonance Imaging
ICA	Independent Component Analysis
ROI	Region of Interest
EEG	Electroencephalography
MEG	Magnetoencephalography
PS	Photic Simulation
COBRE	Center of Biomedical Research Excellence
SP	Schizophrenia Patients
HNV	Healthy Normal Volunteers
AV	Auditory-Visual
A	Auditory
V	Visual
FIFF	Functional Image File Format
MRI	Magnetic Resonance Imaging
ANOVA	Analysis of Variance

FFT	Fast Fourier Transform

Chapter 1

INTRODUCTION

Schizophrenia is a neuro-developmental disorder involving abnormal connections between cortical regions in the brain. Abnormality in these connections leads to misconnections in many aspects of mental activity and hinders the coordination of motor and mental activity. Schizophrenia is a cognitive disturbance and a cognitive deficit that arises from the abnormalities in neural circuits and is defined by the more fundamental disruption in mental processes occurring as a consequence of a disruption in neural circuitry. Thought disorder is the primary defining feature of schizophrenia and exhibits symptoms that represent abnormalities in almost all aspects of human mental activity like inferential thinking, perception, language, motor and social behavior, volition, emotional expression and hedonic capacity etc. [Nancy C. Andreasen, 1999].

Connectivity deficits between various regions of the brain play a major role in the pathophysiology of schizophrenia. A functional magnetic resonance imaging (fMRI) study of schizophrenia using independent component analysis (ICA) identified some networks of the brain which were found to be implicated in schizophrenia during the auditory oddball paradigm. The results of this study indicated that patients with schizophrenia had functional connectivity differences in networks related to auditory processing, executive control and baseline functional activity and also suggested that cognitive deficits associated with schizophrenia are widespread and that a functional connectivity approach can help understand it better [Dae ll Kim et al., 2009.]

Functional Connectivity is defined as the temporal correlation between neurophysiological measurements made in different brain areas. So a pair of regions is considered functionally connected if their activity is in some way correlated. Functional connectivity is caused by the common influence of some external event on distant neural areas and it does not comment on how the correlations between those areas are mediated [Friston et al, 1993].

Coherence is one of the methods for measuring functional connectivity. One characteristic of coherence is that it is insensitive to phase variability across measured time series. In an event-related study, coherence was used to measure the functional connectivity between remote brain regions. It was proposed that coherence was more suitable when phase difference varied largely across brain regions as coherence is less sensitive to such variability. The researchers of this study applied coherence and partial coherence analyses to functional magnetic resonance imaging (fMRI) data to measure task-related functional interactions between neural regions and used this to generate maps of task-specific connectivity associated with seed regions of interest (ROIs). In turn these were compared across tasks, revealing nodes with task-related changes of connectivity to the seed ROI (Sun et al., 2004).

A Functional Magnetic Resonance Imaging (fMRI) study of the functional connectivity throughout the entire brain in schizophrenia found decreased functional connectivity in schizophrenia during rest and also reported that such abnormalities were widely distributed throughout the entire brain rather than restricted to a few specific brain regions. These results strongly supported that schizophrenia may arise from the disrupted functional integration of widespread brain areas [Meng Liang, Yuan Zhou, et al, 2005].

1.1 Magnetoencephalography (MEG)

Magnetoencephalography is a technique for mapping brain activity by recording the magnetic fields produced by the small intra-cellular electrical currents in the neurons of the brain.

Fig 1: MEG System.
Image source:
http://www.unitn.it/en/cimec/10906/magnetoencephalography-lab

MEG is a direct measure of brain activity since it measures the intracellular currents in the neurons. Sensory information sent to the brain causes a nerve impulse which results in an action potential and this action potential causes a small current in the neurons which produces the magnetic fields. The MEG sensors detect these magnetic fields thus recording the brain activity.

These sensors are made of Super Conducting Quantum Interference Devices called SQUIDS which are extremely sensitive to magnetic fields and thus will be able to detect the very weak magnetic fields produced by the intracellular currents in the neurons of the brain. SQUIDS need to be operated at cryogenic temperatures for detection of the weaker magnetic fields and so the SQUIDS are placed in a helmet shaped liquid helium containing vessel called Dewar. To minimize the interference from external magnetic disturbances along with the earth's magnetic field, noise generated by the electrical equipment, radiofrequency signals, and low frequency magnetic fields produced by moving objects, the MEG system is operated in a shielded room. MEG has very high temporal resolution and events with timescales on the orders of milliseconds can be measured. It also has good spatial resolution on the orders of millimeters. MEG is non-invasive and non-hazardous. It does not require injection of isotopes, exposure to X-rays, and exposure to magnetic fields. So children and even infants can be studied using MEG [Hamalainen, et al,. 1993]

1.2 EEG and MEG Coherence

EEG coherence is often used to assess functional connectivity in human cortex. However, moderate to large EEG coherence can also arise simply by the volume conduction of current through the tissues of the head. Volume conduction can elevate EEG coherence at all frequencies for moderately separated (<10 cm) electrodes; a smaller elevation is observed with widely separated (>20 cm) electrodes. This volume conduction effect was readily observed in experimental EEG at high frequencies (40–50 Hz). Cortical sources generating spontaneous EEG in this band are apparently uncorrelated. In contrast, lower frequency EEG coherence appears to result from a mixture of volume conduction effects and genuine source coherence. Surface Laplacian EEG methods help to minimize the effect of volume conduction on coherence estimates by emphasizing sources at smaller spatial scales than unprocessed potentials (EEG). MEG coherence estimates are also affected by the field spread across sources and sensors, however, MEG signals are not as affected by volume conduction as EEG. The type of MEG sensor influences the field spread differently with planar gradiometers limiting field spread more than axial gradiometers or magnetometers [Ramesh Srinivasan et al,. 2007].

1.3 Frequency Bands:

Based on EEG studies, brain activity is often divided into 5 physiologically-based frequency bands. Table 1: Frequency Ranges

Type	**Frequency (Hz)**
Frequency1 - Delta	Up to 4 Hz
Frequency2 - Theta	4 - 8
Frequency3 - Alpha	8 -13
Frequency4 - Beta	>13 - 30
Frequency5 - Gamma	30 - 100+

Source: Niedermeyer E. and Da Silva F.L. (2004). Electroencephalography: Basic Principles, Clinical Applications, and Related Fields. Lippincot Williams & Wilkins. ISBN 0781751268.

Delta frequency band: This frequency band ranges from 0 to 4 Hz. The signals in this frequency have been found during tasks requiring continuous attention.

Theta frequency band: This frequency band ranges from 4 to 8 Hz. The signals in this frequency have been found to rise in situations when a person is trying to hold back a response and also in lot of other situations.

Alpha frequency band: This frequency band ranges from 8 to 13 Hz. The signals in this frequency range arise from occipital regions when eyes are closed and the person is alert and not sleeping. These also arise in different locations across the brain during inhibiting a timing activity.

Beta frequency band: This frequency band ranges from >13 to 30 Hz. Signals in this frequency range are found when a person is cautious and alert working on something with immense concentration.

Gamma frequency band: This frequency band ranges from 30 to above 100 Hz. This frequency range has been implicated in stimulus component binding.

CHAPTER 2

BACKGROUND

2.1 Frequency Specific Deficits:

An EEG study conducted to examine intrahemispheric EEG coherence at rest and during photic stimulation (PS) in 18 drug-naïve patients with paranoid schizophrenia and 30 control subjects reported that schizophrenic patients had significantly higher intrahemispheric coherence of the resting EEG for the delta band compared to that of the controls. This study also reported that during photic stimulation, patients also had significantly higher EEG coherence over the left posterior regions. These results provided evidence that schizophrenic patients have abnormal EEG coherence in both resting and stimulus conditions and suggested more diffuse, undifferentiated functional organization within hemispheres [Yuji Wada et al,. 1998].

Another EEG study with eyes closed in a resting state condition compared the coherence in 11 unmedicated schizophrenic patients (including 9 never medicated patients) and in 15 normal controls and reported that interhemispheric coherence was higher in the patients with schizophrenia in the delta bands in some specific areas of occipital and temporal regions relative to controls [Yaseko Nagase et al, 1992].

These findings provide evidence that schizophrenia patients have frequency specific deficits and have significant differences in the functional connectivity when compared to healthy controls.

Coherence data were estimated from the COBRE project 2 for which my mentor Dr. Julia Stephen was the Principal Investigator. The goal of project 2 was to study the neural mechanisms underlying auditory and visual integration in patients with schizophrenia (SP) and healthy normal volunteers (HNV). My thesis project focused on functional connectivity by analyzing frequency specific deficits between various lobes using MEG coherence as the analysis approach using a task which was specifically designed to study auditory and visual integration in Schizophrenia which involves connectivity between various lobes. Since there are frequency specific deficits reported by researchers previously, I expected to find them between the coherence of Schizophrenics and normal controls while testing for functional connectivity between Left temporal-Parietal, Left temporal-Occipital, Parietal-Occipital, Right temporal-Parietal and Right temporal-Occipital in the delta band frequency using a relatively new procedure of estimating the coherence described in following sections.

2.2 Brain Lobes

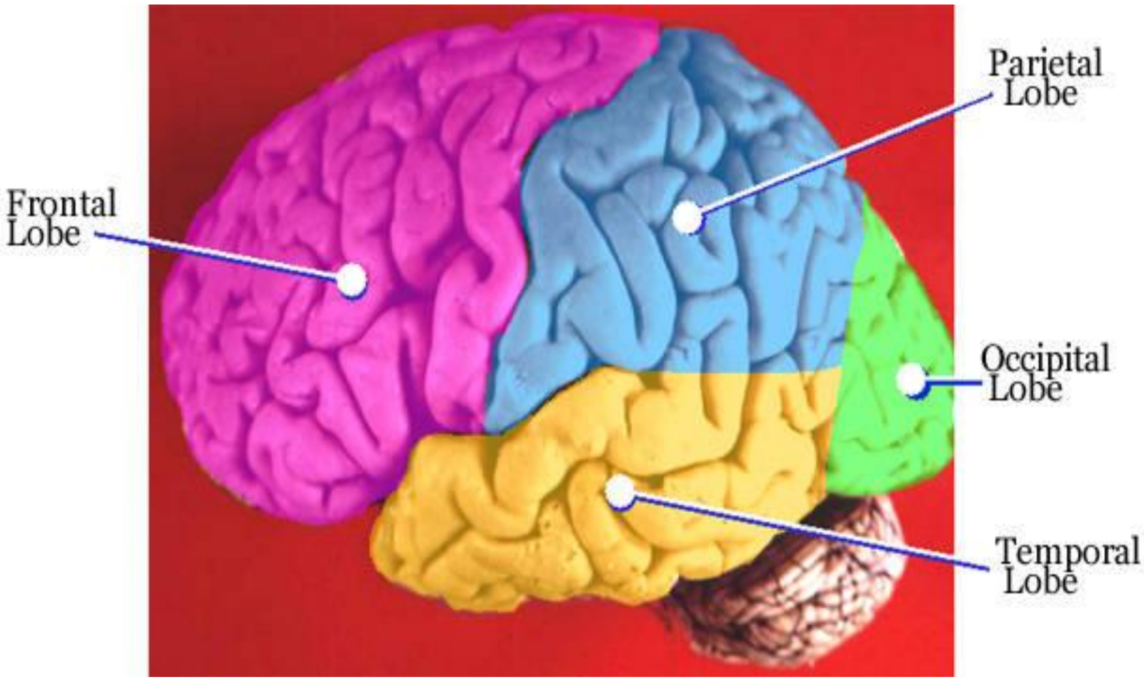

Figure 2: Different lobes of the brain
Image by John A Beal, Louisiana State University, Health Sciences Center Shreveport

Temporal Lobe:

It is located on the bottom section of the brain. Primary auditory cortex which is responsible for interpreting sounds and language we hear is located in this lobe. This lobe is associated with perception and recognition of auditory stimuli, memory, and speech.

Occipital Lobe:

It is located at the back portion of the brain. Primary visual cortex, which receives and interprets information from the retinas of the eyes, is located in this lobe. This lobe is associated with interpreting visual stimuli and information.

Parietal Lobe:

It is located in the middle section of the brain. Somato-sensory cortex which is essential to the processing of the body's senses is located in this lobe. This lobe is responsible for processing tactile sensory information such as pressure, touch, and pain. On the whole it is associated with movement, orientation, recognition and perception of stimuli.

2.3 Task Description:

The MEG data collected for this study was collected during an auditory and visual integration task using an ecologically relevant paradigm that simulates near and distant (far) static sources in a perspective drawing of a soccer field using both auditory and visual stimuli. The stimuli are presented as auditory alone, visual alone, and combined auditory/visual conditions. The subjects must decide whether the stimuli are near or far with a button press. Coherence data were estimated for 6 stimulus conditions. They were S1 - AV Near (Auditory stimulus and Visual stimulus together with the Visual stimulus, a soccer ball appearing near to the subject), S2 - AV Far (Auditory stimulus and Visual stimulus together with the Visual stimulus, a soccer ball appearing far from the subject), S5 - V Near (Visual stimulus alone which is a soccer ball appearing near to the subject), S6 - V Far (Visual stimulus alone which is a soccer ball appearing far to the subject), S7 - A Near (Auditory stimulus alone, which sounds near to the subject) and S8 - A Far (Auditory stimulus alone, which sounds far from the subject).

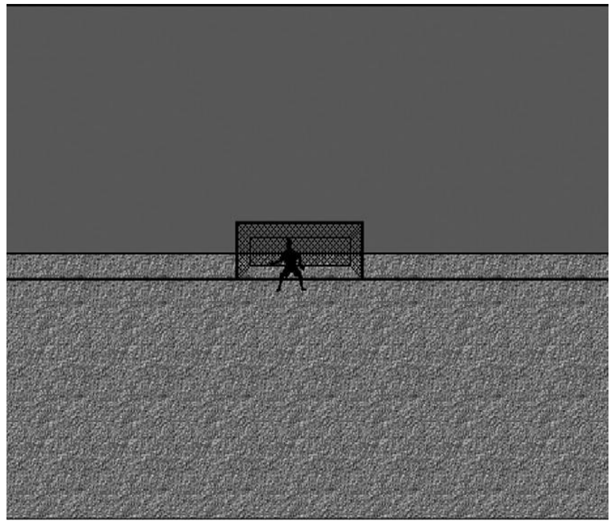

Figure 3: Background perspective drawing of the soccer field with goalie and net. Auditory only stimuli such as ANear and AFar were presented with this background.

Figure 3 shows the back-ground perspective drawing of a soccer field with goalie and net presented for the Audio Near and Audio Far conditions. The background is presented with a brief soccer ball "bouncing" sound (~50 ms duration) with the Audio Near stimulus 6 dB louder than the Audio Far stimulus. The subjects have to decide with a button press whether the stimulus presented is near or far.

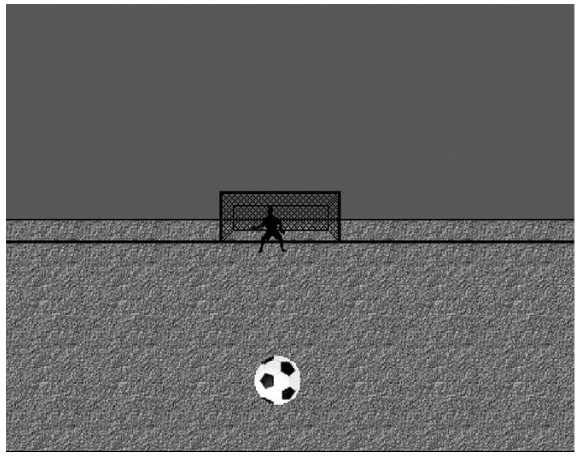

Figure 4: This depicts the Near presentation of visual stimuli Vnear and also for AVNear along with the audio.

Figure 4 shows the back-ground perspective drawing of a soccer field with goalie, net and a soccer ball (appearing near) presented for the Video Near and Audio-Video-Near conditions. The near and far AV stimuli were simulated by offsetting the auditory tone by 5ms relative to the visual stimulus for both near and far conditions.

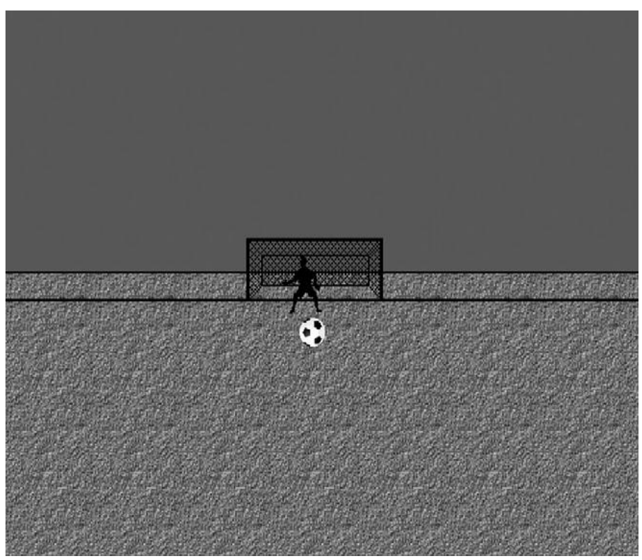

Fig 5: FAR presentation of visual stimuli VFar. This is also shown for AVFar along with an audio. Participants were asked to maintain fixation on the goalie throughout the experiment.

Figure 5 shows the background presented for the Video Far (soccer ball far) and Audio Video Far stimulus conditions.

In the NEAR stimulus condition, the soccer ball appeared in the central foreground of the soccer field and occupied the participant's lower central visual field (visual angle: 0.8◦, eccentricity: 7◦). In the FAR condition, the soccer ball was smaller and occupied the participant's central visual field (visual angle: 0.3◦, eccentricity: 0.5◦). The auditory stimulus was a brief soccer ball "bouncing" sound (~50 ms duration) with the near stimulus 6 dB louder than the far stimulus. For the NEAR and FAR multisensory conditions, auditory and visual stimuli were presented together. All visual stimuli were presented on a computer monitor located 1 m from the participant. Auditory stimuli were presented binaurally through a set of ear inserts.

Fifteen healthy normal volunteers (HNV) and fifteen schizophrenia patients (SP) participated in this study. All participants provided written informed consent, and procedures were conducted in accordance with the standards of the Institutional Review Board of the University of New Mexico and the Declaration of Helsinki.

2.4 Data Processing:

MEG data were collected using the 306 channel MEG machine designed by Elekta Neuromag. Out of 306 channels, 204 channels are gradiometers and 102 channels are magnetometers. After the data collection, data was filtered using Max-filter, a tool designed by Elekta Neuromag to suppress magnetic interferences coming from inside and outside of the sensor array, to reduce measurement artifacts, to transform data between different head positions, and to compensate for disturbances due to head movements (Taulu et al).

Bad channels in the data were manually identified by looking through the data in Neuromag software, Graph, and the identified bad channel numbers were entered into Max-filter. The channels marked in the bad channel tag of the input FIFF-file or manually marked bad in starting MaxFilter are treated as static bad channels, i.e. they are automatically excluded. Maxwell filtering is also applied to improve the standard calibration of MEG systems. The adjustment includes accurately defined sensor orientations and magnetometer calibration factors, and imbalance correction for the planar gradiometers. In addition, cross-talk correction can be applied to reduce mutual interference between overlapping magnetometer and gradiometer loops of a sensor unit.

MaxST in MaxFilter can be regarded as a four-dimensional filter. Besides, the three spatial dimensions it also eliminates artifact in the inner space based on temporal correlations between activity measured in both inner and outer space.

Since head shape and size differs from person to person among the subjects, default head coordinates of (0,0,40) for the center of the head were not used. Instead MRI data of the subject was used. Dicom access was used to convert the mri data files from dicom format to the proprietary Neuromag .fif format. Then Neuromag MriLab tool was used with MRI data in .fif format to calculate the head coordinates for all subjects which are more precise than the default head coordinates of (0,0,40). These coordinates were used for the Max-filter processing to better compensate for disturbances due to head movements. This method allows one to re-interpolate the MEG data to one reference head position reducing the spatial blurring caused by head movement during data collection.

Table 2: Mean age and standard deviations of patients and controls

Diagnosis	Mean	Standard Deviation	Number
Controls	28.93	8.838	15
Patients	38.67	14.465	15
Total	33.80	12.786	30

Patients in this study were undergoing medication during my study and the medication was not the same for all the patients. In order to study the medication effects, Olanzapine equivalent was calculated to bring all the medications to a common scale.

Table 3: Mean Olanzapine equivalent of patients

Patients	Mean Olanzapine Equivalent	Standard Deviation
15	14.02	9.03

CHAPTER 3

COHERENCE METHODOLOGY

3.1 Coherence Methodology:

Classically, EEG recordings of several minutes have been used for coherence analysis, with the data record being divided into a number of overlapping or non-overlapping segments and coherence values then calculated as an average across these segments. The aim of these types of investigations was to study functional connectivity or coupling between different brain areas under various motor, sensory, or cognitive activities. However, studies by Gray and Singer (1989), Gevins (1989), Eckhorn et al. (1988), Roelfsema et al. (1997) have indicated that the coupling between different areas is highly dyamic. The methods involving averaging over some minutes are unable to quantify the short-time evolution of coherence in relation to the specific motor, sensory, or cognitive activity. For this purpose, an event-related paradigm is required, in which the motor, sensory, or cognitive activity (the event) is repeated a number of times under controlled experimental conditions. Coherence values can then be calculated from the ensemble of trials recorded for each repetition of the event, and can yield information that reveals short-time changes in coherence due to the specific cognitive processing involved. This type of event-related processing is known as event-related coherence [Andrew and Pfurtscheller, 1996a,b], [Pfurtscheller, et al, 1999].

In traditional coherence analysis using EEG, brain responses that are evoked by a stimulus or an action are enhanced by averaging the data for each event across epochs.

The underlying assumption is that consistent brain responses exist that are phase locked to a specific event (presentation of a stimulus or motor action).

The magnitude of event-related EEG responses is often several factors smaller than the magnitude of the background ongoing EEG. Therefore, the identification and characterization of these event-related brain responses rely on signal-processing methods for enhancing their signal-to-noise ratio. All these methods require repeating the event of interest a given number of times. The scalp EEG recording is then segmented into epochs, centered around each single event, and all epochs are averaged into a single waveform (time-domain averaging) [12] and [13]. The obtained waveform expresses the average scalp potential as a function of time relative to the onset of the event.

For each condition, stimulation codes from the raw data are detected. Epochs of each stimulus condition are identified and indexes of the beginning of each epoch are found. The mean of each epoch is removed and normalized with the standard deviation to make variance the same. Then all epochs are merged together for the same stimulation code to include all data from one condition in one continuous trial for each channel.

In this approach of estimating coherence by the procedure of merging epochs, coherence analysis was performed for evoked data on one epoch of each stimulation code which is achieved by merging all the epochs and by performing statistical analysis on this epoch.

The amount of phase stability or phase jitter between two different time series is coherence. For two given signals, if the phase difference between them is constant then the coherence is equal to 1, if the phase difference between them is not constant and varies continuously, then the coherence between them is 0.

For two signals at different frequencies, if there is a constant phase difference then the coherence between them is called Cross-Frequency coherence or bi-spectral coherence [Schack et al, 2002; 2005] [Robert W. Thatcher et,al. 2004]. If the two signals are in the same frequency band, then the coherence between them is auto-frequency coherence which is denoted by just coherence. Coherence is amplitude normalized and is a statistic of phase differences. It gives a good estimate of shared energy between mixtures of periodic signals. The importance of coherence lies in the fact that the degree of coupling between two signals cannot be analyzed without depth in the frequency structure over a long period of time. Coherence is also dependent on the consistency of the average of the phase differences between two time series. Coherence also provides the information on the temporal relationship between the coupled signals [Robert W. Thatcher et,al. 2004].

Coherence was estimated by calculating the cross-spectral and power-spectral densities using Welch's modified periodogram averaging method using mscohere function in matlab. Magnitude squared coherence estimate is a function of frequency with values between 0 and 1 that indicates how well x corresponds to y at each frequency. The coherence is a function of the power spectral density (P_{xx} and P_{yy}) of x and y and the cross power spectral density (P_{xy}) of x and y [Kay] [Rabiner et al] [Welch][MathWorks].

$$\boldsymbol{C_{xy}(f) = \frac{\left|P_{xy}(f)\right|^2}{P_{xx}(f)P_{yy}(f)}}$$

4. Results:

Coherence between lobes for AV Near

Left Temporal – Parietal, Fig 6

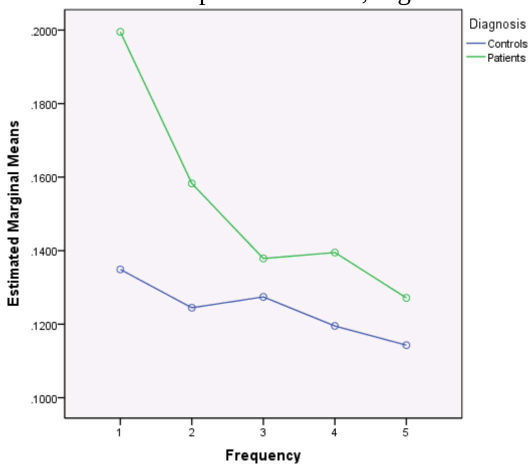

Left Temporal – Occipital, Fig 9

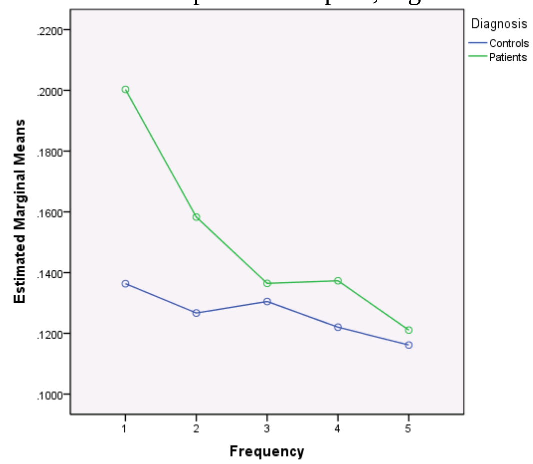

Right Temporal – Parietal, Fig 7

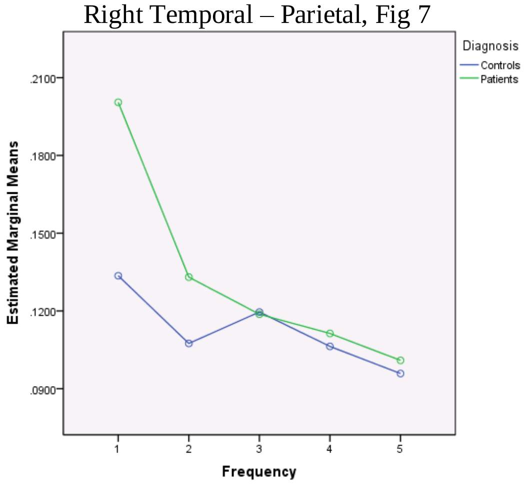

Right Temporal – Occipital, Fig 10

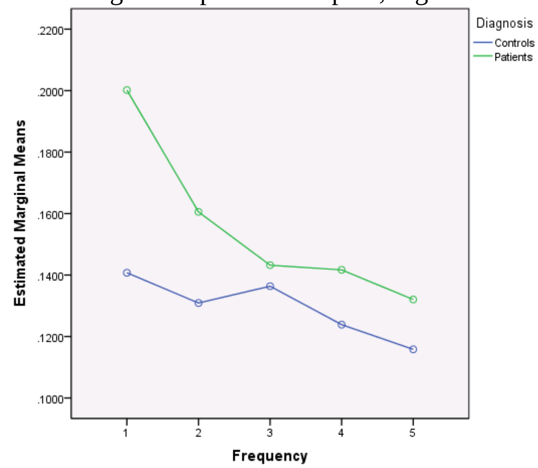

Parietal – Occipital, Fig 8

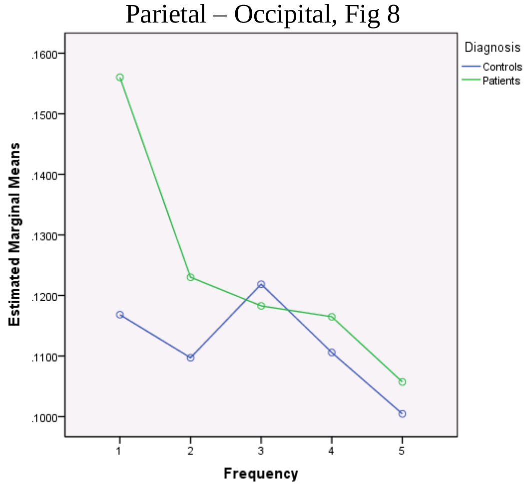

Coherence between lobes for AV Far

Left Temporal – Parietal, Fig 11

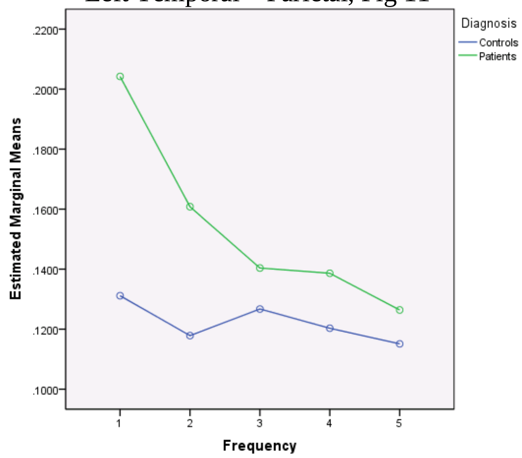

Left Temporal – Occipital, Fig 14

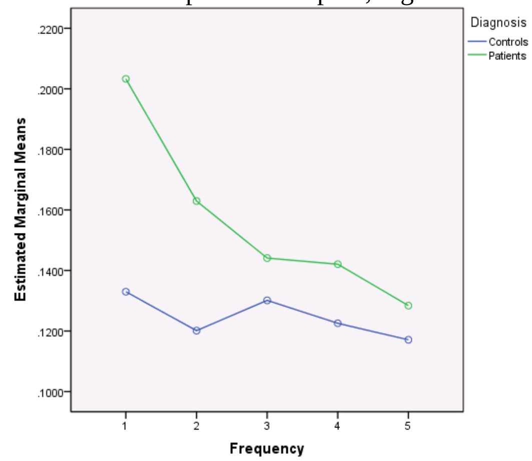

Right Temporal – Parietal, Fig 12

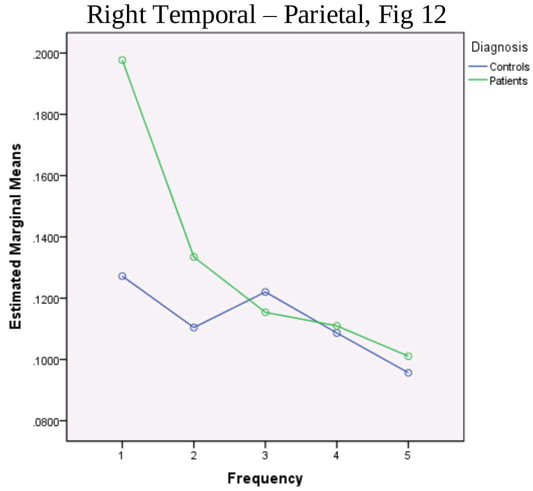

Right Temporal – Occipital, Fig 15

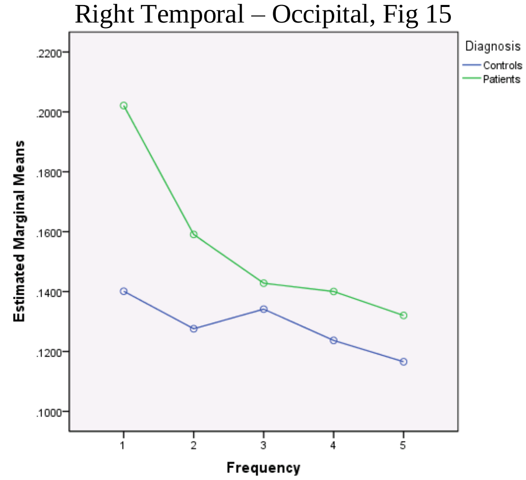

Parietal – Occipital, Fig 13

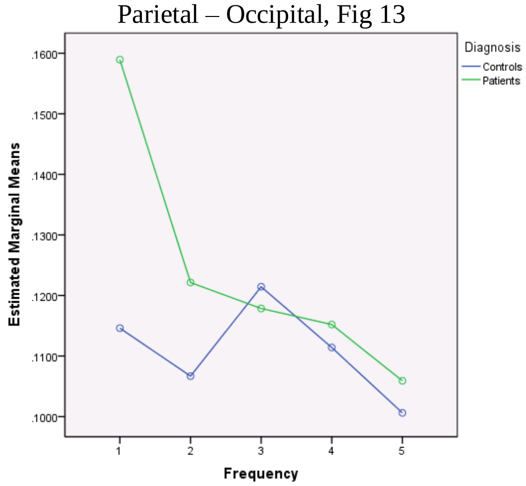

Coherence between lobes for V Near

Left Temporal – Parietal, Fig 16

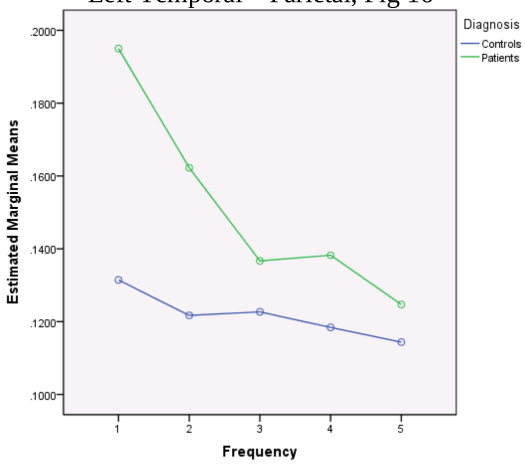

Right Temporal – Parietal, Fig 17

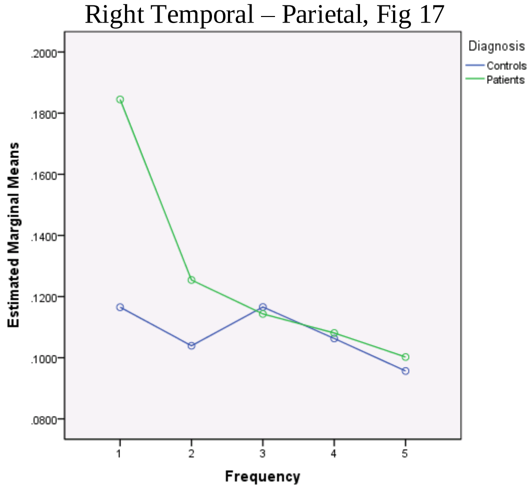

Parietal – Occipital, Fig 18

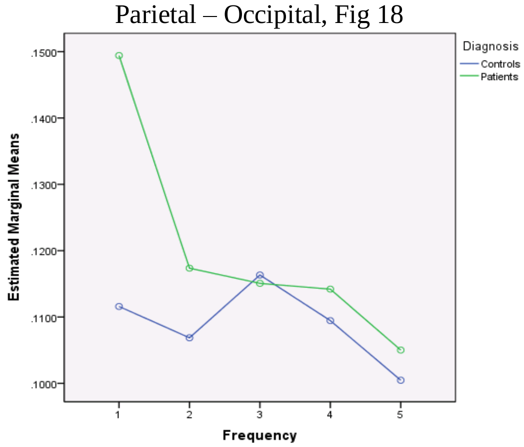

Left Temporal – Occipital, Fig 19

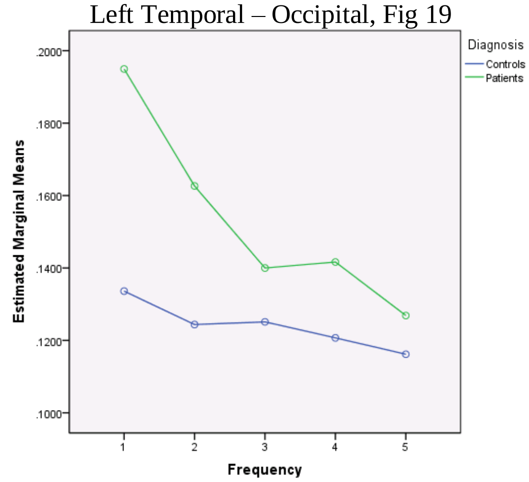

Right Temporal – Occipital, Fig 20

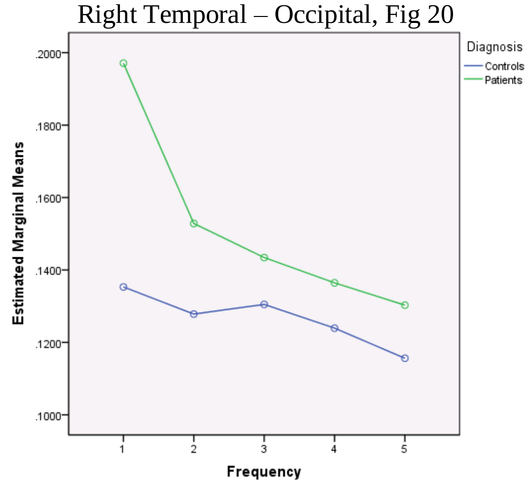

Coherence between lobes for V Far

Left Temporal – Parietal, Fig 21

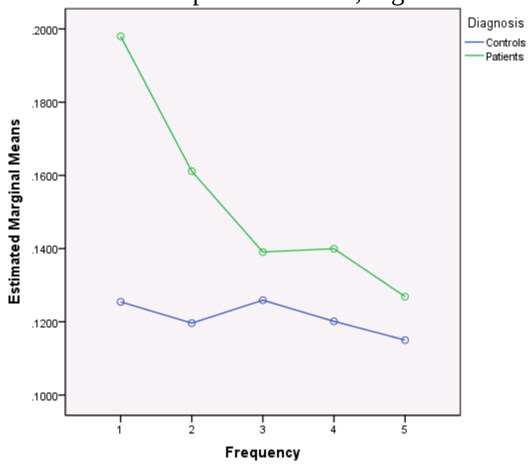

Left Temporal – Occipital, Fig 24

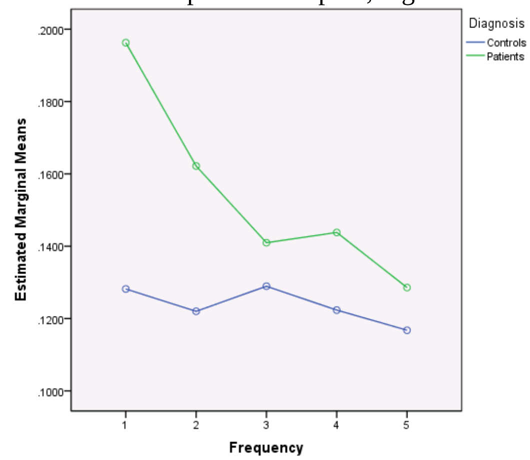

Right Temporal – Parietal, Fig 22

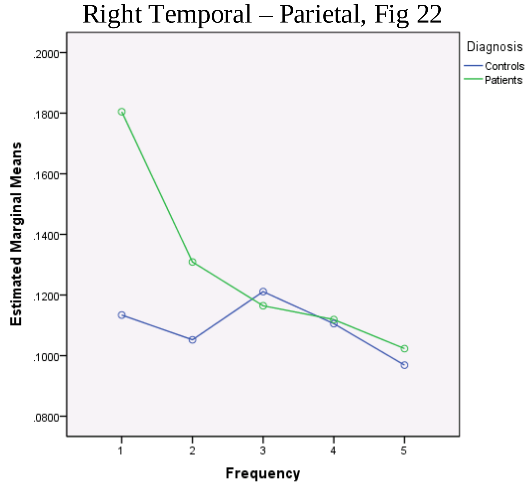

Right Temporal – Occipital, Fig 25

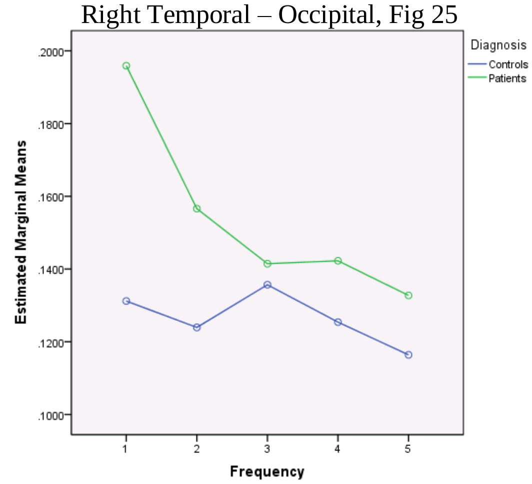

Parietal – Occipital, Fig 23

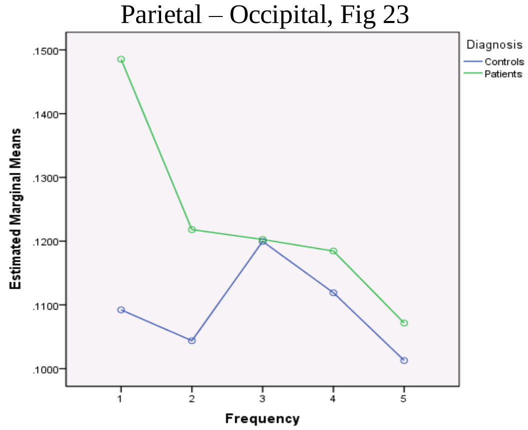

Coherence between lobes for A Near

Left Temporal – Parietal, Fig 26

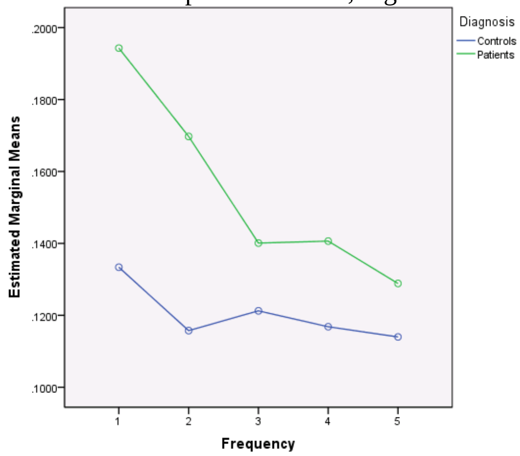

Right Temporal – Parietal, Fig 27

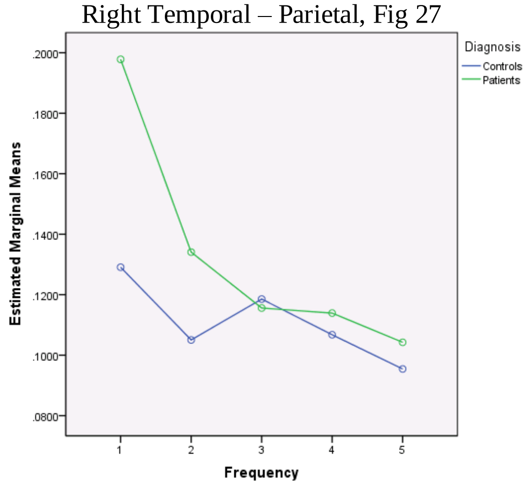

Parietal – Occipital, Fig 28

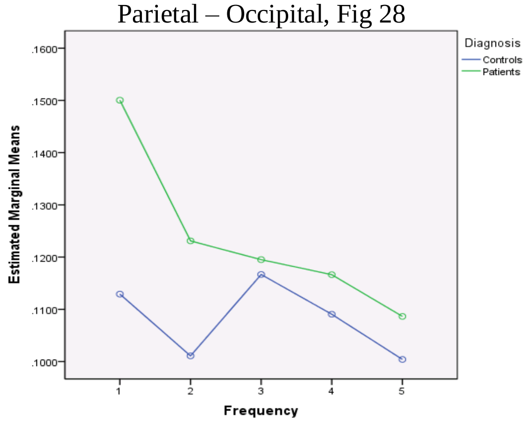

Left Temporal – Occipital, Fig 29

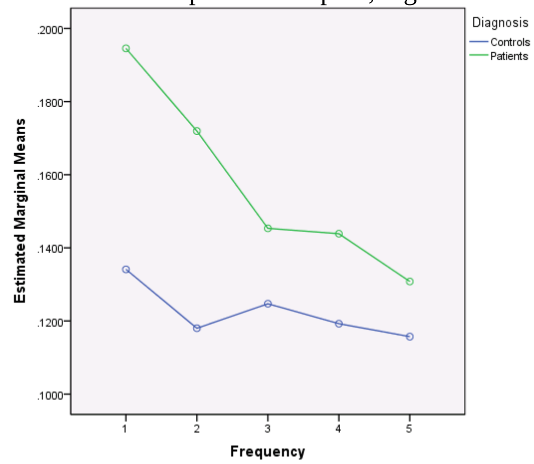

Right Temporal – Occipital, Fig 30

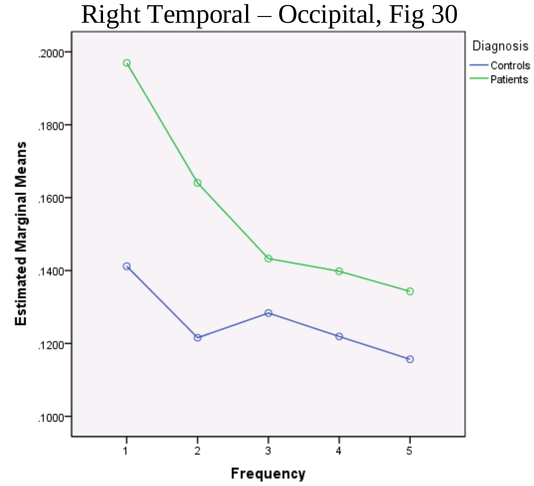

Coherence between lobes for A Far

Left Temporal – Parietal, Fig 31

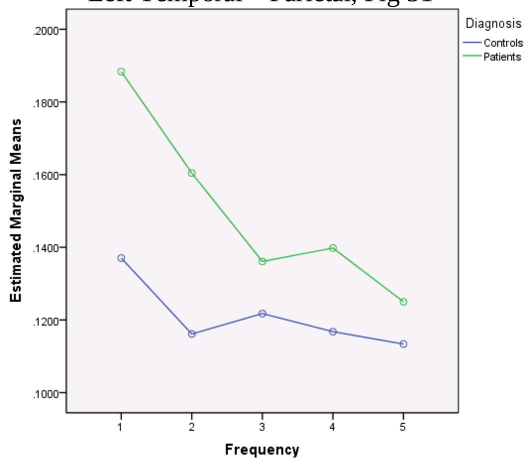

Left Temporal – Occipital, Fig 34

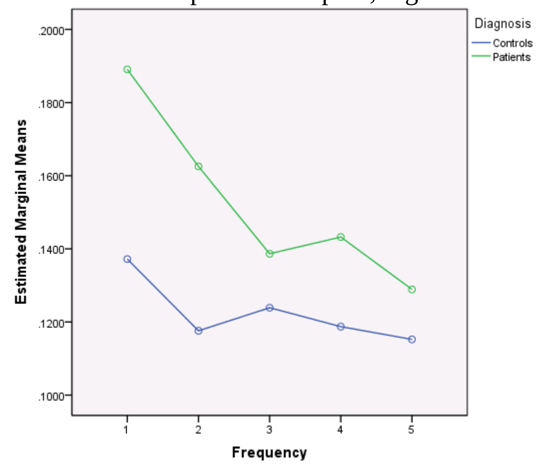

Right Temporal – Parietal, Fig 32

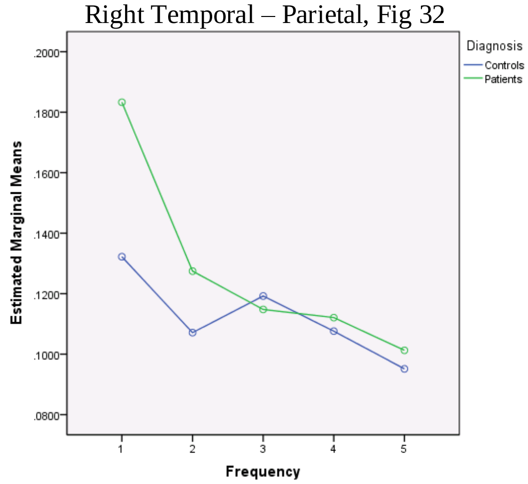

Right Temporal – Occipital, Fig 35

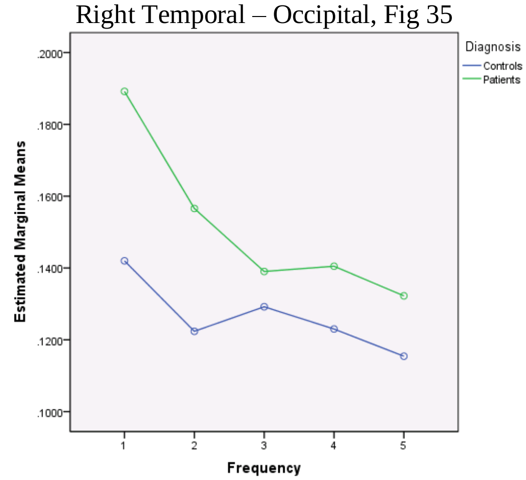

Parietal – Occipital, Fig 33

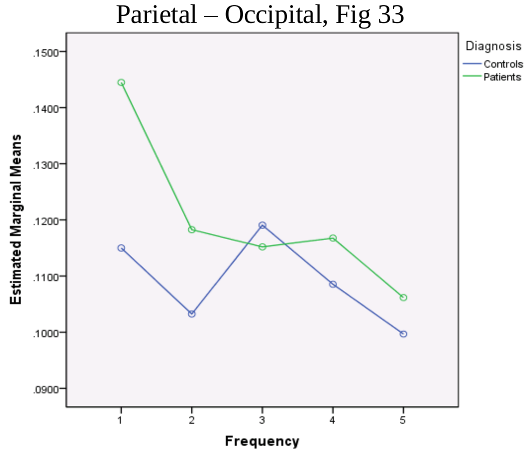

Results:

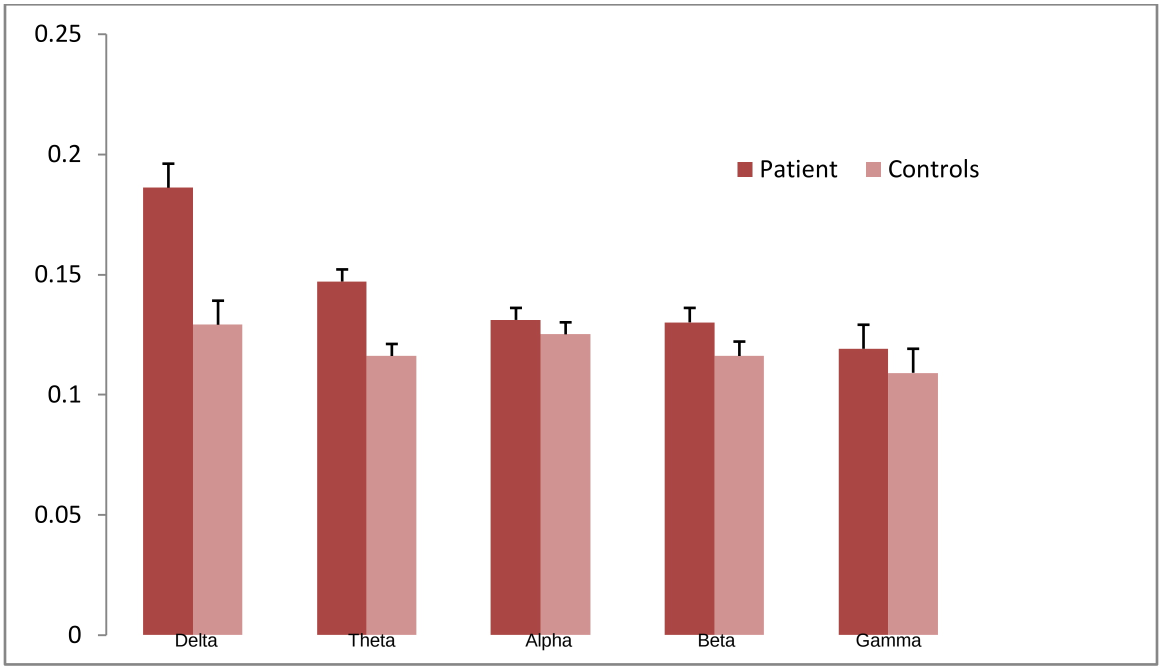

Mean coherence across conditions and regions for each frequency band Fig 36

Analysis Of Variance (ANOVA) was performed on the coherence data of 30 subjects comprised of 15 patients and 15 controls using SPSS. A significant interaction was found between the frequency and diagnosis with age as a covariate $F\ (1, 28) = 5.26, p = 0.003$. Significant differences were found between patients and controls at the Delta frequency band which was confirmed with the Bonferroni-Corrected-t-tests at the delta frequency range in each pair of regions. It was found that patients had higher coherence than controls in the delta frequency band which was quite significant at each pair of lobes for AV Near, AV Far, V Near, V Far, A Near and A Far stimulus conditions.

CHAPTER 5

CONCLUSION

5.1 Conclusion:

These results agreed with the results reported by other studies [Yuji Wada et al,. 1998] [Yaseko Nagase et al, 1992] on the delta band frequency deficits in schizophrenia between patients and controls where patients exhibited higher coherence in the delta band than controls which suggests that patients with schizophrenia have abnormal MEG coherence in stimulus conditions and suggest differences in the functional organization and connectivity between various lobes of the brain.

Studies by Gray and Singer (1989), Gevins (1989), Eckhorn et al. (1988), Roelfsema et al. (1997) have indicated that the coupling between different areas is highly dynamic. The methods involving averaging over some minutes are unable to quantify the short-time evolution of coherence in relation to the specific motor, sensory, or cognitive activity and reported that event-related paradigm is required, in which the motor, sensory, or cognitive activity (the event) is repeated a number of times under controlled experimental conditions. So this project employed event related paradigms during the data collection for a robust analysis of coherence to understand the functional connectivity and frequency specific deficits.

Study by [Yaseko Nagase et al,. 1992] has reported patients having higher coherence than controls in delta band frequency in unmedicated patients in schizophrenia. Since the patients in my study were undergoing medication, the results of my study indicate that there exist delta band frequency specific deficits in medicated patients also. Medication level was one the major difference between my project and other studies [Yaseko Nagase et al, 1992]. Furthermore, previous studies [Yaseko Nagase et al, 1992] reported frequency specific deficits in the Delta band using resting state data instead of an event related paradigm.

The coherence analysis methodology used in this project is also different from the other studies mentioned in the literature survey. In traditional analysis of coherence, the coherence analysis was performed on each epoch of evoked data and then the statistics were performed. In my project, there was a one single long epoch for each stimulus condition on which coherence analysis was performed and then statistical analysis was performed to test for significance. This approach saves time and computer resources compared to traditional approach on which analysis has to be performed on each and every epoch of each stimulus condition.

The limitation of this work is that exact locations of the functional connectivity deficits are yet to be identified in each of the lobes. Due to the time constraint, this will be studied in the future work of this project. Also, data of only 30 subjects (15 controls and 15 patients) was used in the project. A larger dataset will help us to better understand the functional connectivity and frequency specific deficits between the controls and patients. More work has to be done to understand the advantages and disadvantages of this new approach for coherence analysis.

5.2 Future Work:

My next focus is going to be to understand the correlation of the medication and symptoms based on the frequency band differences and to compare different measures of functional connectivity with coherence. My future work is to better understand the advantages and disadvantages of the new coherence approach relative to the traditional method and to increase the datasets for the controls and patients for more robust results. Due to the exhausting and time consuming manual process of estimating coherence, I used the data of 15 controls and 15 patients. I will be working to automate the process of estimating coherence so that I can use a larger dataset to better understand the frequency specific deficits and the complex process underlying the functional connectivity between the lobes at a greater detail and also to exactly quantify how much time this approach saves when compared to traditional analysis of coherence. My plan also is to work to estimate the coherence between evoked multisensory and summed unisensory responses and compare the similarities and differences to gain a better understanding of the roles, the different frequency bands play in integration of multisensory stimuli. Finally, coherence estimates obtained after source analysis will provide more specific information about the source of the connectivity deficits in schizophrenia.

Appendix:

Coherence shows the measure of how much two sets of time series resemble each other with values ranging from 0 (not resembled at all) to 1 (perfectly resembled). Coherence gives a measure of phase consistency or synchrony between two signals at a particular frequency. Phase consistency which indicates higher coherence suggests evidence for “anatomical connections” (Fein et al., 1988), “functional coupling” (Thatcher, 1986), “information exchange” (Petsche et al.,1992), “functional coordination” (Gevins et al., 1989), and “temporal coordination” (Gray and Singer, 1989) between the cortical structures underlying these areas. Mathematically, coherence is analogous to a cross-correlation coefficient in a frequency domain. It shows the frequencies at which two sets of time series data are coherent and at which frequencies they are not. Coherence is a cross spectral density function normalized by the product of power spectral density functions of both time series. Power spectral density function (PSD) shows the strength of the variations (energy) as a function of frequency. It shows at which frequencies variations are strong and at which frequencies variations are weak. Energy within a specific frequency range is obtained by integrating the power spectral density function (PSD) within that frequency range. PSD is computed by Fast Fourier Transform (FFT) or by computing autocorrelation function and then transforming it. Cross spectral density is a Fourier transform of cross correlation function and also can be computed by Fast Fourier Transform [Pfurtscheller et al,. 1999] [Cygnus Research International].

$$C_{xy}(f) = \frac{|P_{xy}(f)|^2}{P_{xx}(f)P_{yy}(f)}$$

Coherence can be calculated with the calculation of auto-spectrum and cross-spectrum [Thatcher et,al. 2004]. Auto-spectrum is a measure of the amount of energy or activity at different frequencies. Cross-spectrum is the energy in a frequency band that is in common to the two different raw data time-series. Coherence is the normalization of the cross-spectrum which is the ratio of the auto-spectra and cross-spectra. The FFT of a signal is a complex number containing real and imaginary parts. The power in each frequency component represented by FFT is obtained by squaring the magnitude of that frequency component. The power in k^{th} frequency component which is the k^{th} element of FFT is given by the following equation.

Power = $|X[k]|^2$

Where $|X[k]|$ is the magnitude of the frequency component.

The power is obtained by squaring the magnitude of the FFT, so FFT which gives a complex output must be used since it also has phase information.

Power Spectrum $S_{AA}(f) = \frac{FFT(A) * FFT^{*}(A)}{N^2}$

Where $FFT^{*}(A)$ denotes the complex conjugate of FFT(A) and the complex conjugate of FFT(A) results from negating the imaginary part of FFT(A).

Cross Power Spectrum $S_{AB}(f) = \frac{FFT(B) * FFT(A)}{N^2}$

When signals A and B are the same, then the power spectrum is equivalent to the cross power spectrum and so power spectrum is often referred to as the auto power spectrum or the auto spectrum.

The amount of energy present at a specific frequency band is autospectrum. It was shown by Fourier that autospectrum can be computed by multiplying each point of the raw data by a series of cosines, and independently again by a series of sines, for the frequency of interest. The average product of the raw-data and cosine is known as the cosine coefficient of the finite discrete Fourier transform and the average product of the raw-data and sine is known as the sine coefficient. These cosine and sine components express the relative contributions of each frequency. The basic constituents of all spectral calculations are these cosine and sine constituents. For a real sequence {$x_{i,}$ i = 0, ……..,N-1} where Δt is a sample interval and f_i is the frequency, then the cosine and sine transforms are calculated as:

Cosine Coefficient = a(n) = $\Delta t \sum_{i=1}^{N} (\mathrm{X(i)} \cos 2\pi \mathrm{fi} \Delta t)$

Sine Coefficient = b(n) = $\Delta t \sum_{i=1}^{N} (\mathrm{X(i)} \sin 2\pi \mathrm{fi} \Delta t)$

The average cosine coefficient = a(n) = $1/N \sum_{i=1}^{N} \left(\mathrm{X(i)} \cos(\frac{2\pi f i}{N})\right)$

The average sine coefficient = b(n) = $1/N \sum_{i=1}^{N} \left(\mathrm{X(i)} \sin(\frac{2\pi f i}{N})\right)$

The power spectral value for any frequency intensity is given by

F(x) = (a^2(x) + b^2(x)) which is the sum of the squares of the sine and cosine coefficients at each frequency.

The in-phase and out-of-phase components of the signals of A and B are important for the calculation of cross-spectrum. The in-phase components are referred to as cospectrum and the out-of-phase components are referred as quadspectrum. Sine coefficients and Cosine coefficients of signals A and B are used in the computation of the in-phase component. The out-of-phase component is calculated by relating the cosine coefficient of time series A to the sine coefficients of B and similarly the sine coefficients of time series A to the cosine coefficient of time series B.

For any two in-phase sine waves, the quadspectrum is zero which means the phase difference is zero. Mathematically, cospectrum and quadspectrum are calculated as:

Cospectrum (f) = x(a) u(b) + y(a) v(b)

Quadspectrum(f) = x(a) v(b) – y(a) u(b) where

x(a) = cosine coefficient for the frequency f, for channel A

y(a) = sine coefficient for the frequency f, for channel A

u(b) = cosine coefficient for the frequency f, for channel B

v(b) = sine coefficient for the frequency f, for channel B

Cross-spectrum power = $\sqrt{(\text{Cospectrum}(f)^2 + \text{Quadspectrum}(f)^2)}$

The absolute value of the complex-valued cross-spectrum is the cross-spectrum power. The measure of connectivity based on the total shared energy between two locations at a specific frequency is the cross-spectrum power which is a mixture of in-phase and out-of-phase components. Since the complex number times the complex conjugate is a real number, the cross-spectrum power is a real number. Coherence is a normalization of the cross-spectral power by dividing by the autospectra and therefore, coherence is independent of autospectral amplitude or power and varies from 0 to 1.

$$\text{Coherence}(f) = \frac{|\text{Cross-Spectrum}(f)AB|^2}{(\text{Autospectrum}(f)(A))(\text{Autospectrum}(f)(B))}$$

References:

Wolfgang H. R. Miltner, Christoph Braun, Matthias Arnold, Herbert Witte and Edward Taubs. Coherence of gamma-band EEG activity as a basis for associative learning. Nature, Vol 397, Feb 4th, 1999.

Nancy C. Andreasen. A Unitary Model of Schizophrenia. Arch Gen Psychiatry, Vol 56, Sep 1999. www.archgenpsychiatry.com.

Andreasen NC. The role of the thalamus in schizophrenia.Can J Psychiatry. 1997;42:27-33.

Andreasen NC. Linking mind and brain in the study of mental illness: a project for a scientific psychopathology.Science. 1997;275:1586-1593.

Andreasen NC, Paradiso S, O'Leary DS. Cognitive dysmetria as an integrative theory of schizophrenia: a dysfunction in cortical-cerebellar circuitry? Schizophr Bull. 1998;24:203-218.

K.J. Friston, C.D. Frith, P.F. Liddle, and R.S.J. Frackowiak. Functional Connectivity: The Principal-Component Analysis of Large (PET) Data Sets. Journal of Cerebral Blood Flow and Metabolism, 13:5 – 14, 1993.

Meng Liang, Yuan Zhou, Tianzi Jiang, Zhening Liu, Lixia Tian, Haihong Liu and Yihui Hao. Widespread functional disconnectivity in schizophrenia with resting-state functional magnetic resonance imaging. Brain Imaging, Vol 17, No 2 February 2006.

Julia P. Owen, David P. Wipf, Hagai T. Attias, Kensuke Sekihara and Srikantan S. Nagarajan. Robust methods for reconstructing brain activity and functional connectivity between brain sourceswith MEG/EEG data. Biomedical Imaging: From Nano to Macro, 2009. ISBI '09. IEEE International Symposium; 1945-7928:1271 – 1274;

URL: http://ieeexplore.ieee.org/stamp/stamp.jsp?arnumber=05193294

Felice T. Sun, Lee M. Miller, and Mark D'Esposito. Measuring interregional functional connectivity using coherence and partial coherence analyses of fMRI data. NeuroImage 21 (2004) 647–658;

URL:http://www.sciencedirect.com/science/article/pii/S1053811903006062

Deborah J. Serrien, Richard B. Ivry & Stephan P. Swinnen. Dynamics of hemispheric specialization and integration in the context of motor control. Nature Reviews Neuroscience 7, 160-166 (February 2006);

Saad, Z. S., Ropella, K. M., Cox, R. W., and DeYoe, E. A. (2001). Analysis and use of FMRI response delays. *Hum. Brain Mapp.* 13, 74–93.

Miezin, F. M., Maccotta, L., Ollinger, J. M., Petersen, S. E., and Buckner, R. L. (2000). Characterizing the hemodynamic response: effects of presentation rate, sampling procedure, and the possibility of ordering brain activity based on relative timing. *Neuroimage* 11, 735–759.

Fornito A, Yoon J, Zalesky A, Bullmore ET, Carter CS. General and Specific Functional Connectivity Disturbances in First-Episode Schizophrenia During Cognitive Control Performance. Biol Psychiatry. 2011 Apr 21;

D. Kim , J. Burge , T. Lane , G.D. Pearlson , K.A. Kiehl , V.D. Calhoun. Hybrid ICA–Bayesian network approach reveals distinct effective connectivity differences in schizophrenia. NeuroImage 42 (2008) 1560–1568.

Yuji Wada, Yuko Nanbu, Mitsuru Kikuchi, Yoshifumi Koshino, Takuma Hashimoto. Aberrant functional organization in schizophrenia: analysis of EEG coherence during rest and photic stimulation in drug-naive patients.Neuropsychobiology 1998;38:63-69.

Nicholas D. Davenport, BA; Kelvin O.Lim, MD; Scott R. Sponheim. Intrahemispheric EEG Coherence related to Fractional Anisotropy in Schizophrenia.

Yuri Koh, Kyung Soon Shin, June Sic Kim, Jung-Seok Choi, Do-Hyung Kang, Joon Hwan Jang, Kwang-Hyun Cho, Brian F. O'Donnell, Chun Kee Chung, Jun Soo Kwon. An Meg study of alpha modulation in patients with Schizophrenia and in subjects at high risk of developing psychosis. Schizophrenia Research 126 (2011) 36 – 42 pages.

Julia M. Stephen, Cheryl Aine, Vincent Clark, Robert Freedman. Auditory and Visual Integration in Schizophrenia Examined Using MEG, EEG and fMRI.

Ramesh Srinivasan, William R. Winter, Jian Ding, Paul L. Nunez. EEG and MEG coherence: Measures of functional connectivity at distinct spatial scales of neocortical dynamics. Journal of Neuroscience Methods 166 (2007) 41-52.

Yaseko Nagase, Yoshira Okuba, Masato Matsuura, Takuya Kojima and Michio Toru. EEG coherence in unmedicated schizophrenic patients: Topographical study of predominantly never medicated cases. Biological Psychiatry Volume 32, Issue 11, December 1992, pages 1028-1034.

Robert W. Thatcher, Carl J. Biver and Duane M. North. EEG and Brian Connectivity: A Tutorial. Applied Neuroscience Research Institute and Applied Neuroscience Laboratories.MaxFilter User's Guide, Software Version 2.0, October 2006.

P. Bucci, A. Mucci, E.Merlotti, U. Volpe and S. Galderisi. Induced Gamma Activity and Event-Related Coherence in Schizophrenia. Clinical EEG and Neuroscience; April 2007; 38, 2; ProQuest Central. Pg. 96.

L. Marzetti, S. Della Penna, G. Nolte, R. Franciotti, G. Stefanics, G.L. Romani. A Cartesian Time-Frequency Approach to Reveal Brain Interaction Dynamics. Brain Topogr (2007) 19:147-154.

A. Mouraux, G.D. Iannetti. Across-trial averaging of event-related EEG responses and beyond. Magnectic Resonance Imaging 26 (2008) 1041-1054.

Kay, S.M. *Modern Spectral Estimation*. Englewood Cliffs, NJ: Prentice-Hall, 1988. Pg. 454.

Rabiner, L.R., and B. Gold. *Theory and Application of Digital Signal Processing*. Englewood Cliffs, NJ: Prentice-Hall, 1975.

Welch, P.D. "The Use of Fast Fourier Transform for the Estimation of Power Spectra: A Method Based on Time Averaging Over Short, Modified Periodograms." *IEEE Trans. Audio Electroacoust*. Vol. AU-15 (June 1967). Pgs. 70-73.

Andrew CM, Pfurtscheller G. Event-related coherence as a tool for studying dynamic interaction of brain regions. Electroencephalogr Clin Neurophysiol 1996; 98: 144-8.

Andrew CM, Pfurtscheller G. Dependence of coherence measurements on EEG derivation type. Med Biol Eng Comp 1996; 34:232-8.

Gray CM, Singer W. Stimulus-specific neuronal oscillations in orientation columns of cat visual cortex. Proc Nat Acad Sci USA 1989;86:1698-702.

Gevins AS, Cutillo BA, Bressler SL. Morgan NH, White RM, Illes J, Greer DS. Event-related covariances during a bimanual visuomotor task II: Preparation and feedback. Electroencephalogr Clin Neurophysiol 1989;74:147-60.

Eckhorn R, Bauer R, Jorgan W, Brosch M, Kruse W, Munk M, Reitboeck HJ. Coherent oscillations: a mechanism of feature linking in the visual cortex? Biol Cybern 1988;60:121-30.

Roelfsema PR, Engel AK, Konig P, Singer W. Visuomotor integration is associated with zero time-lag synchronization among cortical areas. Nature 1997;385:157-61.

Pfurtscheller, Gert, Andrew and Colin. Event-Related Changes of Band Power and Coherence: Methodology and Interpretation. Journal of Clinical Neurophysiology, Issue: Volume 16(6), November 1999, p 512.

Fein G, Raz J, Brown FF, Merrin EL. Common reference coherence data are confounded by power and phase effects. Electroencephalogr Clin Neurophysiol 1988;69:581-4.

Cygnus Research International - http://www.cygres.com/OcnPageE/Glosry/Spec.html

Cygnus Research International - http://www.cygres.com/OcnPageE/Glosry/Coh.html

Petsche H, Lacroix D, Lindner K, Rappelsberger P, Schmidt-Henrich E. Thinking with images or thinking with language: a pilot EEG probability mapping study. Psychophysiology 1992;12:31-9.

Thatcher RW, Krause PJ, Hrybyk M. Cortico-cortical associations and EEG coherence: a two compartmental model. Electroencephalogr Clin Neurophysiol 1986;64:58-75.

Schack, B., Vath, N., Petsche, H., Geissler, H.G. and Moller, E. Phasecoupling

of theta-gamma EEG rhythms during short-term memory processing. Inst. J. Psychophysiol., 44:143-163, 2002.

Schack, B., Klimesch, W. and Sauseng, P. Phase synchronization betweentheta and upper alpha oscillations in a working memory task. Int. J. Psychophysiol., 57: 105-114, 2005.

http://www.mathworks.com/help/toolbox/signal/ref/mscohere.html

www.4dneuroimaging.com

http://www.nmr.mgh.harvard.edu/martinos/research/technologiesMEG.php

Matti Hamalainen, Riitta Hari, Risto J. Iimoniemi, Jukka Knuutila, and Olli V. Lounasmaa. Magnetoencephalography – theory, instrumentation, and applications to noninvasive studies of the working human brain. Reviews of Modern Physics, Vol. 65, No. 2, April 1993.

S. Taulu, M. Kajola, and J. Simola. Suppression of interference and artifacts by the signal space separation method. *Brain Topography* **16**(4), 269-275, 2004.

S. Taulu, and M. Kajola. Presentation of electromagnetic multichannel data: the signal space separation method. *Journal of Applied Physics*, **97**(12), 124905, June 2005.

S. Taulu, J. Simola, and M. Kajola. Applications of the signal space separation method. *IEEE Transactions on Signal Processing*, **53**(9), 3359-3372, 2005.

S. Taulu, and J. Simola. Spatiotemporal signal space separation method for rejecting nearby interference in MEG measurements. *Physics in Medicine and Biology*, **51**, 1759-1768, 2006.